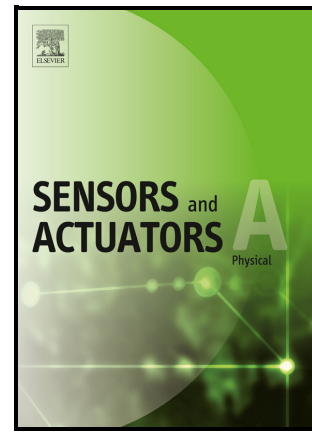


Recognition of metallic and semiconductor single-wall carbon nanotubes using the photoelectric method

A.V. Kozinetz, S.V. Litvinenko, B.B. Sus, A.I. Manilov, A.S. Topchylo, A. Rozhin, V.A. Skryshevsky



PII: S0924-4247(21)00573-2

DOI: <https://doi.org/10.1016/j.sna.2021.113108>

Reference: SNA113108

To appear in: *Sensors and Actuators: A. Physical*

Received date: 16 February 2021

Revised date: 27 August 2021

Accepted date: 9 September 2021

Please cite this article as: A.V. Kozinetz, S.V. Litvinenko, B.B. Sus, A.I. Manilov, A.S. Topchylo, A. Rozhin and V.A. Skryshevsky, Recognition of metallic and semiconductor single-wall carbon nanotubes using the photoelectric method, *Sensors and Actuators: A. Physical*, (2021) doi:<https://doi.org/10.1016/j.sna.2021.113108>

This is a PDF file of an article that has undergone enhancements after acceptance, such as the addition of a cover page and metadata, and formatting for readability, but it is not yet the definitive version of record. This version will undergo additional copyediting, typesetting and review before it is published in its final form, but we are providing this version to give early visibility of the article. Please note that, during the production process, errors may be discovered which could affect the content, and all legal disclaimers that apply to the journal pertain.

© 2021 Published by Elsevier.

Recognition of metallic and semiconductor single-wall carbon nanotubes using the photoelectric method

A.V. Kozinetz^{1,}, S.V.Litvinenko^{1,2}, B. B. Sus¹, A.I. Manilov¹, A.S.Topchylo¹, A.Rozhin³, V.A. Skryshevsky^{1,2}*

1 Institute of High Technologies, Taras Shevchenko National University of Kyiv

2 Corporation Science Park Taras Shevchenko University

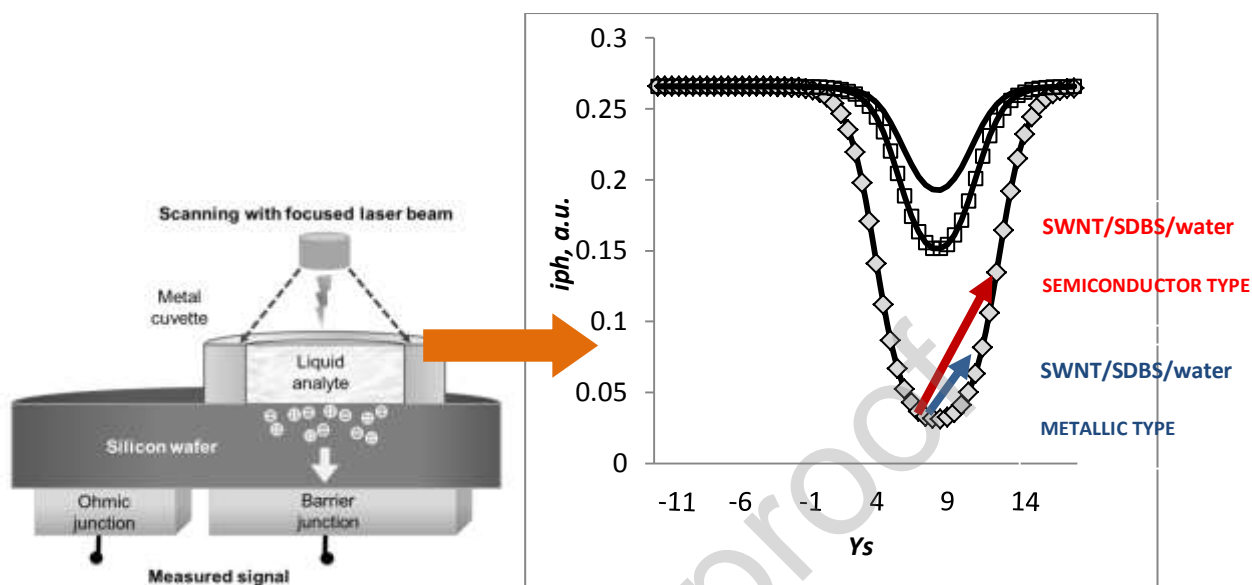
3 Aston University

*Correspondent author alk22k@gmail.com

Abstract—an innovative application of deep barrier silicon structures for sensory devices with photoelectrical transformation has been suggested. The principal possibility of the photovoltaic transducer implementation for identification of metallic and semiconductor single-wall carbon nanotubes covered with surfactant in water solution was analyzed in detail. The obtained results are qualitatively explained by local electrostatic influence on the parameters of recombination centers at the silicon surface. This influence can be associated with the dipole moment of molecules absorbed at the surface of the nanotube from surfactant sodium dodecylbenzene sulfonate (SDBS). Moreover, the spatial configuration of charged fragments near the defects at the silicon surface can occur. Another possible reason for carbon nanotubes identification is due to the different polarizability of metallic and semiconductor nanotubes. These results are explained in the frame of Stevenson-Keyes's theory. The reported effect can be further applied as the basis for the control and selection of carbon nanotubes with different conductivity types.

Keywords — silicon surface, carbon nanotube composites, sensor application

Graphical Abstract



1. INTRODUCTION

The single-wall carbon nanotubes (SWNT) form a one-dimensional class of carbon nanomaterials. They can be represented as graphene sheets “rolled up” to form hollow tubes which wall is only one atom thin [[1],[2],[3]]. The typical diameter of nanotubes is 0.5-4 nm whereas the length can be 10~1000 times greater. The (SWNT) is considered a very promising modern material due to its extraordinary physical and mechanical properties. Potentially it can be used in various biomedical applications (drug delivery, bioimaging, DNA sensors), in microelectronic (transistors for computing, conductive transparent composites, light-emission panel), for hydrogen storage and composite material [[4],[5],[6],[7]]. It is known that by the means of functionalization, the SWNT tends to interact with certain chemical compounds or biological objects. The covalent, noncovalent, or external decoration with inorganic nanomaterial can be regarded as a modification of the surface reactivity of carbon nanotubes. The optical properties and conductivity type significantly depend on the direction of the “rolling up” of hexagonal graphene lattice. The latter, in turn, determines their diameter and allows the classification of SWNT symmetry by chirality indices [8, 9].

Several principal methods can be implemented for the synthesis of nanotubes, such as the thermal plasma method, chemical vapor deposition, or liquid electrostatic method [10]. Unfortunately, the SWNTs dispersed in water tend to agglomerate due to strong van der Waals interactions. To achieve the solubility of hydrophobic nanotubes in water, a special surfactant should be added. The molecule of the surfactant realizes non-covalent functionalization due to π - π stacking interaction with the graphitic surface of the nanotube. The resulting substations are a mixture of tubes of different chirality, some of which are metallic and semiconducting types. It should be noted that it is acceptable to select certain types of tubes for functional applications [11,12]. That is why a certain post-synthesis procedure of tube solving, separation, and purification is required. The fact that nanotubes of semiconductor types are more hydrophobic is frequently used in different separation methods. So, separation of SWNTs with different conductivity types can be implemented using density-gradient centrifugation, dielectrophoresis, selective interaction with surfactants, or selective covalent functionalization [[13],[14],[15]]. All these procedures can be successfully implemented for the development of new material and their application, including the tubes of a certain type in a polymer matrix. The metallic and semiconducting tubes demonstrate different chemical reactivity. The field-effect transistors were created by deposition of individual tubes grown from patterned islands on SiO_2/Si substrate. The conductivity of the semiconductor tube channel is very sensitive to electrical gating. It can be changed by orders of magnitude under gate voltages and exposure in HN_3 and NO_2 atmospheres. On the contrary, metallic types are less sensitive to chemical adsorption because charge transfer does not affect the carrier density near the Fermi level [2].

Given that obtaining the selected fraction with a certain type of conductivity is an important technological purpose, some additional control methods should be applied [16, 17]. Currently, this control can be implemented by applying different optical (photoluminescence measurement, Raman spectroscopy) or electro physical techniques. The sensory structure based on a deep silicon barrier was recommended for the detection of different substances containing the molecular structures with their own or induced dipole moment [[18],[19],[20]]. The operation principle of sensory structure is based on the photocurrent dependence on the effective surface

recombination at the silicon surface. To investigate the peculiarities of the absorption process at the silicon surface it is necessary to measure the photocurrent through the barrier structure. It was shown that this type of photovoltaic transformation is very sensitive to the local electric field near the effective surface. In the present work, the possibility developing the physical base for recognition of the SWNT type has been discussed in detail. It is considered that such an approach can be useful to develop simple additional instruments for controlling the type of tube conductivity. At the same time, functionalized nanotubes can be hazardous due to their toxicity and ability to pass through the biological barriers in cells [[21],[22],[23]]. Therefore, it is important to develop new methods for detecting such substances. The problems of the physical properties of silicon interface should be also considered since they determine the solid state electronic progress. That is why investigation of SWNT interaction with silicon surface is another objective of the presented research.

2. EXPERIMENT

In our studies, deep silicon barrier structures were used to study the peculiarities of SWNT adsorption. In such a way the transducer with photoelectrical conversion principle was realized with metal-silicon contact. Silicon wafers (100) with *p*-type conductivity and specific resistance of 40-50 $\Omega \cdot \text{cm}$ (carrier concentration consist 10^{15} cm^{-3}) were chosen.

It was determined that the photocurrent of deep silicon barrier structure depends on surface recombination significantly when light with high absorption coefficient is used [21] (in other words the area where light is absorbed and the space charge region should be spatially separated). The simplified expression for photocurrent collected from *p*-base of deep barrier structure is

$$i_{ph}(S) \cong \frac{1 + \frac{S}{\alpha(\lambda)D}}{S \frac{l}{D} \operatorname{sh}\left(\frac{d}{l}\right) + ch\left(\frac{d}{l}\right)} \quad (1)$$

where D is an electron diffusion ratio, $\alpha(\lambda) \sim 10^5 \text{ cm}^{-1}$ ($1/\alpha(\lambda) \sim 0.1 \mu\text{m}$), S – surface recombination rate, d - the thickness of *p*-Si wafer. In our experiments $d = 300 \mu\text{m}$, l - the electron diffusion length is about $150 \mu\text{m}$. To obtain 2D photocurrent distribution, the surface of the silicon substrate was scanned by a laser beam

with $\lambda = 532$ nm wavelength. The light spot was moved on the sample surface, addressing discrete spots to form a 512×512 elements matrix. The deflection of the laser beam was achieved with the system of acoustic-optical crystals. With the implementation of a metal cuvette (volume of the cuvette is 0.1 mL) a solution contact with the surface can be achieved, Fig.1. As wafer thickness is much more than $1/a(\lambda)$ value, the incident light is absorbed near the upper surface, distant from the space charge region. So, the principal conditions for sensory structure are fulfilled in our experiments. No additional treatment was applied to the effective surface covered by a film of native oxide SiO_x . The proposed experimental system can be implemented for the analysis and comparison of the photocurrent 2D distributions of through the barrier junction during the illumination of the surface with the analyte.

The single-wall carbon nanotubes were manufactured by South West Nano Technologies (SWeNT®). Two types of SWNT produced by Co-Mo CAT catalytic technologies [24] were investigated in detail: 1) the first - SG 65, enriched in chirality (6, 5), was characterized by semiconductor conductivity (the semiconductor tubes content is nearly 90%), average diameter 0.7 nm; 2) the second - CG 200, was characterized metal conductivity (metallic tube content up to 80%), average diameter 0.7-1.4 nm.

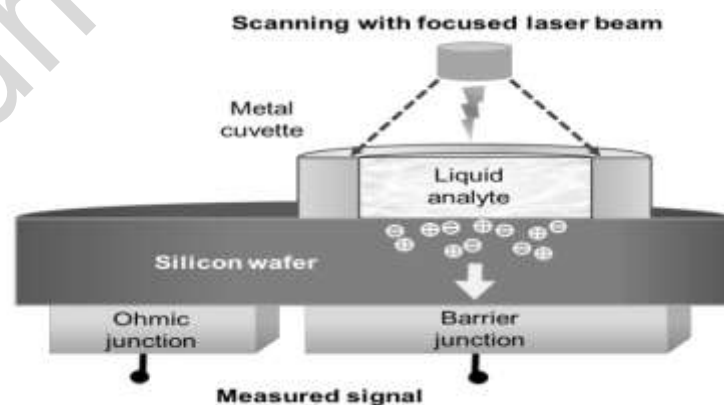


Fig. 1. Schematic image of the sensory structure and cuvettes with an analyte

Both investigated solutions contain 1.2 mg of high purity SWNT and 12 mg of surfactant sodium dodecylbenzene sulfonate (SDBS). The SDBS stabilizes nanotubes in a wide range of diameters. The ultrasonic sonication was used to

disperse bundles of carbon nanotubes; the resulting suspension was further centrifuged on a Beckman Coulter Optima Max-XP (MLS 50) for 2 hours. The procedure provides the adsorption of surfactant on the surface of SWNT and supports the formation of time-stable transparent colloidal solutions. The water solutions with the same concentrations of nanotubes and surfactants were prepared. The absorption spectra in the visible and near infra-red range were measured using a Lambda 1050 UV/VIS/NIR spectrometer. The emission spectra at various excitation wavelengths were recorded using a Horiba NanoLog excitation-emission fluorometer equipped with an InGaAs array detector to generate photoluminescence (PL) maps.

The size distributions and zeta potential of carbon nanotubes are studied with the Malvern Zetasizer device. The characteristic size of carbon nanotubes is estimated to be nearly 100 nm for both solutions. The measured values of zeta potential of SG 65 and CG 200 are respectively - 40 mV and -39 mV. The negative values of zeta potential are typical for carbon nanoparticles in the organic solvent [25]. The obtained values of zeta potential indicate the relative stability of carbon nanotubes in the solvent at ambient temperature without coagulation tendency.

3.RESULTS AND DISCUSSION

3.1 Simplified model of photoelectrical sensor

Initially, the model of sensory structure based on a deep silicon barrier should be considered. Several steps are necessary to make (1) accessible for practical implementation. It is appropriate to analyze the possible functional dependencies of S on the pre surface band bending Y . This analysis can be done in the frame of Stevenson-Keyes theory taking into account the single simple recombination level in the bandgap, Fig.2. In such a case the surface recombination velocity S is [26]:

$$S(Y_s) = \frac{c_p c_n N_t (p_0 + n_0)}{c_n (n_s(Y_s) + n_i) + c_p (p_s(Y_s) + p_i)}, \quad (2)$$

where n_0 and p_0 are equilibrium carrier concentrations in the volume; $n_1 = n_i \exp(E_{ti}/kT)$, and $p_1 = n_i \exp(-E_{ti}/kT)$ are the carrier concentrations when Fermi level at the surface is equal to the energy of recombination level E_{ti} at the surface counted from the middle of band gap; $c_n = \sigma_n v$, $c_p = \sigma_p v$ are the capture cross-sections, v is the electron (hole) thermal velocity; n_i is intrinsic concentration, N_t is

the concentration of recombination centers, where the dependence between surface and volume concentrations can be expressed as: $n_s = n_o \exp(Y_s/kT)$ and $p_s = p_o \exp(-Y_s/kT)$. The parameter $e\phi$ at the diagram in Fig.2 characterizes the doping level in volume of wafer. It is easy to show that $e\phi = kT \ln(p_o/n_i)$. The equilibrium hole concentration in the volume of wafer was set at $p_o = 10^{15} \text{ cm}^{-3}$, so the $e\phi$ value equals to 0.3 eV.

For better representation of possible physical conditions associated with the analyte adsorption, the series of the $S(Y_s)$ dependencies were determined according to (2). The changes of the microscopic recombination centers parameters, i.e. value of E_{ti} , c_n and c_p , were analyzed. The calculations results are presented in Fig. 3, 4. It is well known, that typical $S(Y_s)$ dependence is presented by bell-shaped curve.

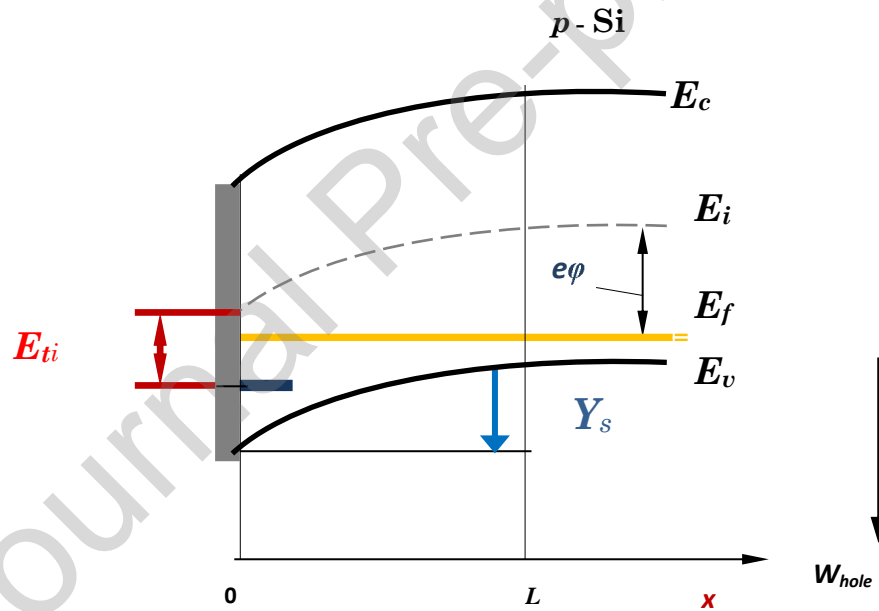


Fig. 2 The energy diagram of pre surface region in p -Si wafer (the energy of simple single recombination level is marked as navy-blue stripe). The L is width of space charge region.

The maximum of the dependence corresponds to equation

$$c_n n_s = c_p p_s \quad (3).$$

In general, the equation (3) can be evaluated from the $dS/dY=0$ extremum condition. The maximum recombination velocity is

$$S_{max} \sim 0.5 (c_n c_p)^{1/2} N_t ((p_o + n_o)/n_i) / (1 + ch((E_{ti}/kT) - \ln(c_p/c_n)^{1/2})) \quad (4),$$

where the corresponding band bending is - $Y_{smax} = kT \ln(c_p/c_n)^{1/2}(p_o/n_i)$.

The recombination rate increases when Fermi level gets close to the middle of the band gap. As for the decrease of recombination rate related to ranges $Y_s \leq Y_{smax}$ and $Y_s \geq Y_{smax}$, the effect can be explained by the absence of carrier of a certain sign in pre surface region when the silicon surface is driven from the flat band through depletion into inversion condition. The Fig. 3 illustrates the case of equal capture cross-section $c_n=c_p=c$ (“neutral recombination center”). As can be seen from these dependencies, the closer the energy of recombination level E_{ti} is to the middle of band gap, the less wide the bell-shaped curves become. This feature is related to the impact of the exponential factor $\exp(E_{ti}/kT)$ in (2). Actually, we can express

$$S(Y_s) = \frac{cN_i(p_o + n_o)}{n_s(Y_s) + n_i + p_s(Y_s) + p_i} \approx \frac{cN_i(p_o + n_o)}{n_s(Y_s) + p_s(Y_s) + n_i e^{E_{ti}/kT}} \quad (5).$$

It easy to see, that while surface band bending provides the $n_s(Y_s), p_s(Y_s) < n_i \exp(E_{ti}/kT)$ conditions, the “plateau” near the maximum of $S(Y_s)$ is observed. In other words, a higher value of the E_{ti} allows keeping the conditions in a wider range of Y_s and the wider “plateau” is observed. For the curves in Fig. 3, the parameter of energy level E_{ti} is varied from $10kT = 0,25$ eV to $2kT = 0.05$ eV. As can be seen, the peak of the recombination velocity S_{max} for curves 1-5 corresponds to the same value of band bending $Y_{osmax} = e\phi = kT \ln(p_o/n_i) = 9KT \sim 0.3$ eV. In the frame of suggested model, doping level and conductivity type completely define the band bending corresponding to maximal recombination. The Y_{osmax} should provide the condition of equal concentrations near surface, i.e. $n_s = p_s = n_i$ (p_s should be less than volume concentration p_o , while n_s should be greater than n_o for p -type silicon wafer). It can be also noted that increase of E_{ti} involves decrease of maximal recombination as $S_{max} \sim 1/(1 + ch(E_{ti}/kT))$, Fig.3 (insertion).

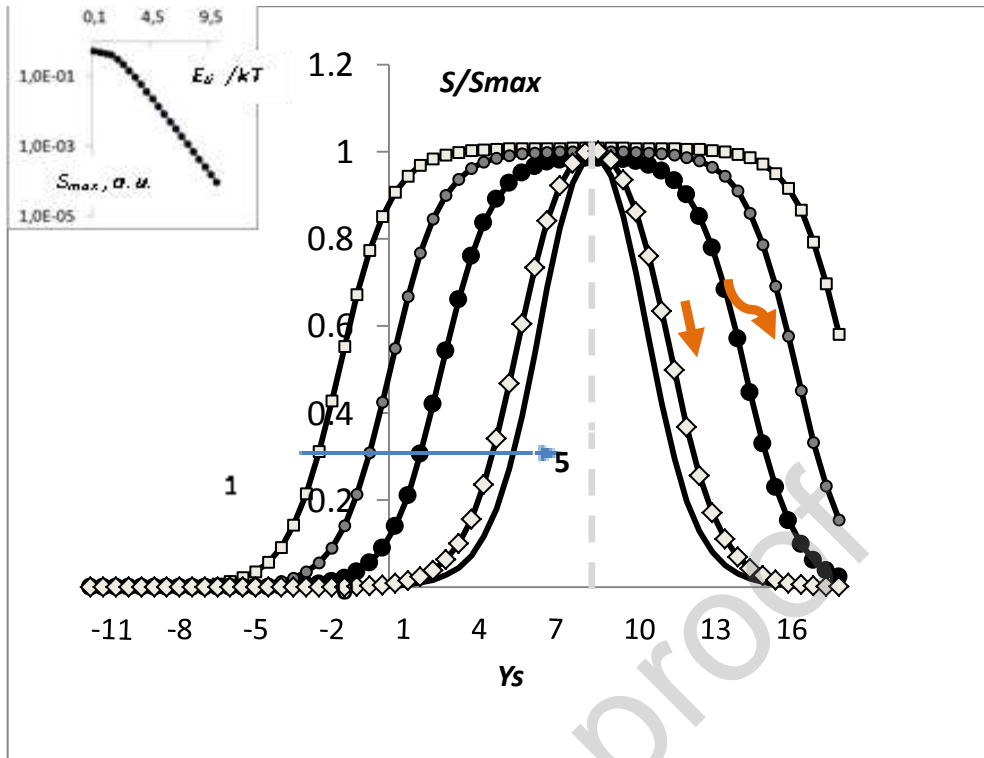


Fig. 3 The calculated surface recombination velocity versus surface band bending for different values of energy level E_{ti} : $10kT$ (1), $8kT$ (2), $6kT$ (3), $3kT$ (4), $2kT$ (5). Insertion: the calculated maximal recombination rate versus energy level. Doping level of p -Si wafer is 10^{15} cm^{-3} . The dependence of maximal recombination rate on energy level E_{ti} is presented in insertion.

So, when the condition of $E_{ti}/kT \geq 1$ is continued, the simplified expression takes place $S_{max} \sim \exp(-E_{ti}/kT)$. Instead of a simple single recombination level, the continuous systems of donor and acceptor recombination levels can occur at the interface. The numerical simulation reveals that the “deformation” of the bell-shaped curves is quite possible in this case for high injection levels [27]. However, the main conclusion is as follow: when close concentrations of carriers are generated near surface - the recombination velocity gets its maximal value; if the lack of carriers of certain sign takes place-recombination velocity decrease.

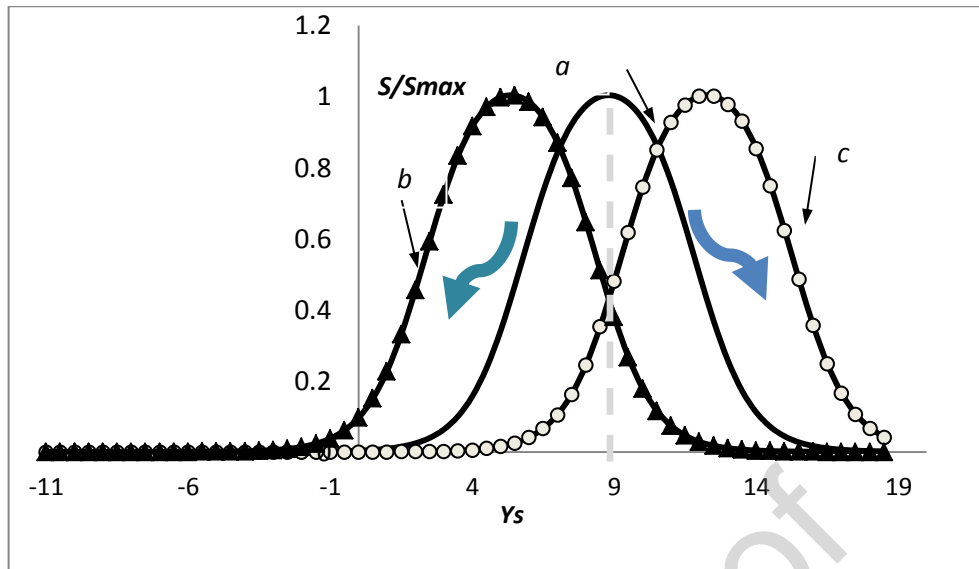


Fig.4. The calculated surface recombination velocity versus surface band bending for the different ratios of cross- sections: $c_p=c_n$ (a), $c_p=10^{-3} c_n$ (b), $c_p=10^3 c_n$ (c), for all cases $E_{ti}=3kT=0.075$ eV.

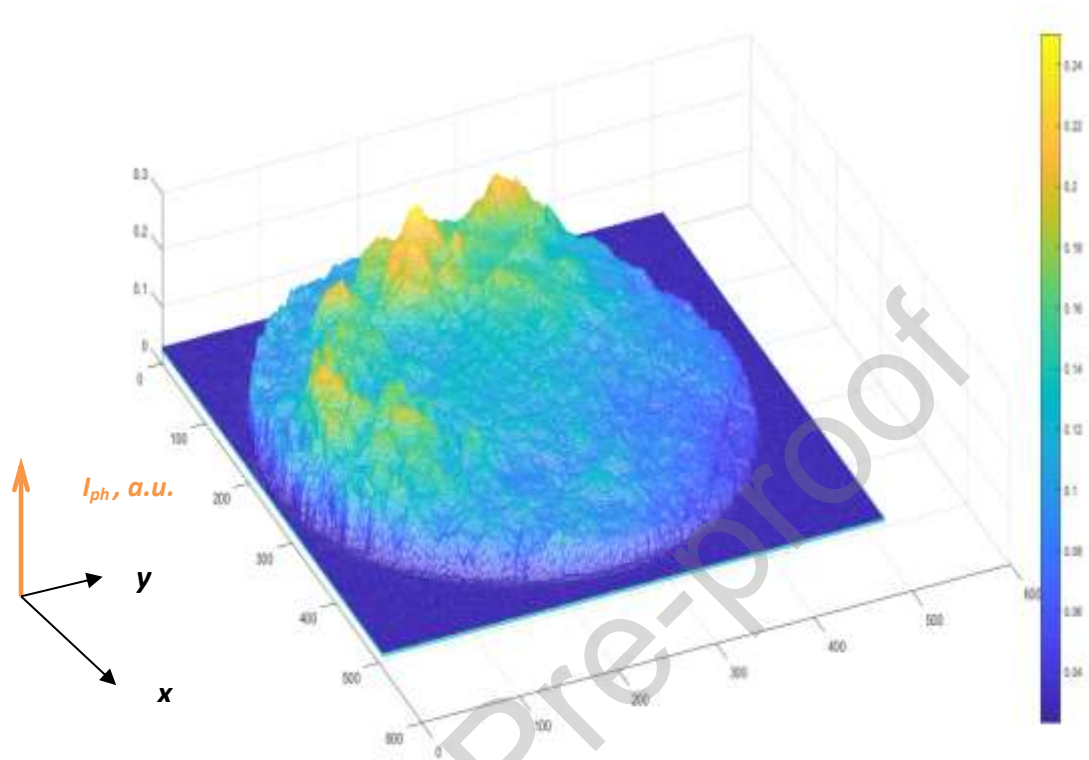
The other case is when cross-sections become different from each other $c_n \neq c_p$, (shown in Fig.4). It is supposed that surface contact with polar molecules provides the condition when neutral centers exhibit donor- or acceptor-like properties. The energy value $E_{ti}=3kT=0.075$ eV is maintained for all curves. When, for example, $c_p=10^{-3}c_n$, as is appropriate for “donor-like center”, the maximum of $S(Y_s)$ corresponds to lower band bending $Y_{(1)}$ (curve b) because the condition (4) requires higher value of p_s . When $c_p=10^3c_n$, as it can be appropriate for “acceptor-like center”, higher band bending $Y_{(2)}$ (curve c) is needed to get the holes concentration providing a maximum of recombination. The dependences b) and c) are in some sense symmetrical relative to the axis $Y=Y_{o\ max}$ (curve a) which corresponds to $c_n=c_p$. The deviation of $Y_{(1),(2)}$ from this axis is equal to $\pm 0.5kT \ln(c_p/c_n)$. As can be seen, higher differences between c_p and c_n should correspond to higher $|Y_{(1),(2)} - Y_{o\ max}|$ value. In absolute units, the deviation is nearly $4kT=0.1$ eB for the case discussed above. So, it can be seen that shifting of the curve is sensitive to the change of the cross-sections ratio. Therefore, we can suppose that the change of surface recombination may be related to band bending via different functional dependences. Namely, if recombination centers parameters (cross-sections, energy) rest unchanged, one of the “bell-shaped” curves shown in Fig. 3 describes the functional dependence. If carrier cross-sections or energy of recombination level are influenced by the local electric field, the “transfer” between two curves takes place

(stripes in Fig.3, 4). Considering some analogy with well-known sensory structures based on field-effect transistor (FET), we suppose that local electrical fields change primarily the surface band-bending. In some cases, this process may be accompanied by changes of each recombination parameter. Such a scenario is implemented, for example, if the system of levels (discrete or continuous) exists at the interface. The value of recombination rate changes when “Fermi level at the surface” passes through the energy of certain recombination level, i.e. when $Y_s = e\phi - E_{ti}$, Fig. 2. It means that increasing Y_s leads to the fact that several levels ($E_{ti}^{(1)}$, $E_{ti}^{(2)}$,...) influence the peculiarities of the recombination process. Consequently, several sets of parameters (E_{ti} , N_t , c_n , c_p) should be considered in the sensor model. If energy bands between such levels is sufficiently high ($\geq kT$), several maximums of recombination velocity $S(Y_s)$ are expected to observe. The suggested approach allows us to obtain the dependences of photocurrent on surface parameters for deep barrier structures, section 3.3.

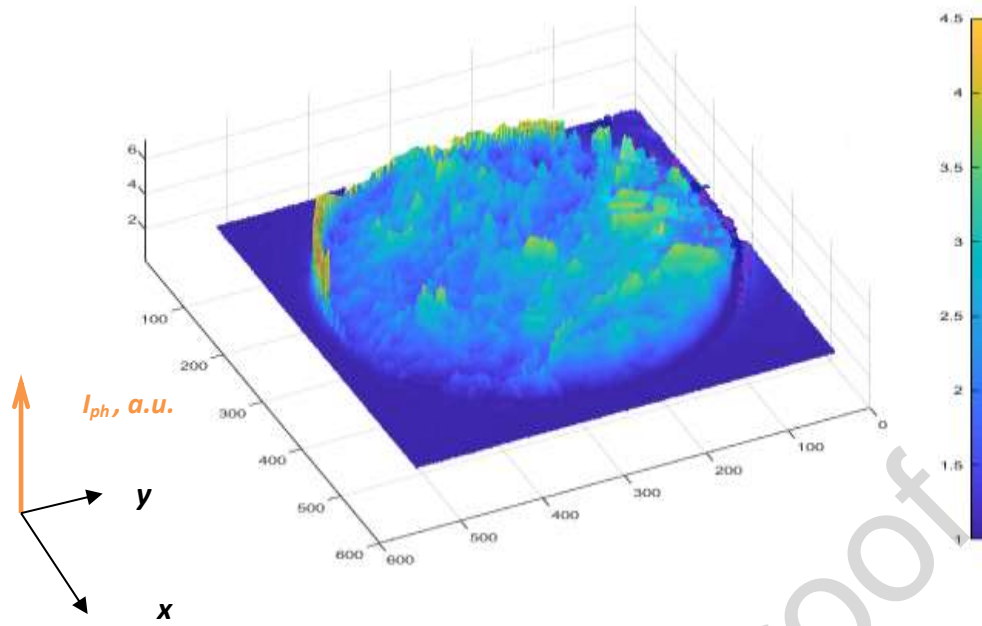
3.2 Experimental results and characterization of SWNT water solutions

The 2D distribution of photocurrent was experimentally measured for three cases: 1) the silicon surface contacting with ambient air, 2) the silicon surface contacting with the solution of SWNT of semiconductor type - SG 65, 3) the silicon surface contacting with the solution of SWNT of metallic type - CG 200. The obtained results were treated statistically. The possible error is determined by standard set-up allowing photocurrent measurement. It consists of several per cent. Each of the three series includes at least ten measurements of 2D distribution. The silicon surface was cleaned with distilled water after each contact with the analyte. The good reproducibility of experimental results was observed. The averaged results are presented in Fig. 5. As can be observed from Fig. 5 a) the non-uniform distribution of photocurrent $I_{ph}(x, y)$ is obtained for silicon surface without analyte. This fact is naturally attributed to different initial band bending Y_0 and different recombination rate in each illuminated points (x, y) of the surface. The distributions of normalized photocurrent for SG 65 and CG 200 are presented in Fig.5 b) and Fig.5 c). The normalization to the value for photocurrent in ambient air was applied. The increase of photocurrent is observed for the two analytes, but this increase is significantly more pronounced for SG 65 solution (the ratio $I_{ph}^{sg65}(x, y) / I_{ph}(x, y)$ is 2.5-3.5), than for CG 200 (the ratio $I_{ph}^{cg200}(x, y) / I_{ph}(x, y)$ is 1.5-1.7. All

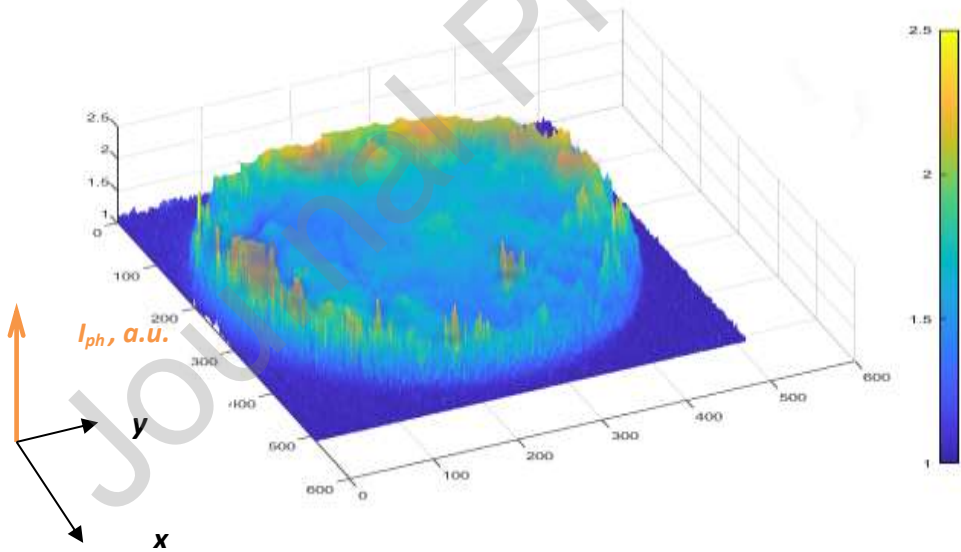
these effects can be explained by the decrease of surface recombination at the silicon surface, registered through the photocurrent measurement.



a)



b)



c)

Fig. 5 The 2D distribution of photocurrent for silicon surface contacting with ambient air (a), solution of SWNT of semiconductor type (b), solution of SWNT of metallic type CG 200 (c). The normalization to the values of photocurrent in ambient air was applied for distributions (b) and (c),

In other words, the suggested sensory structure can be used for the identification of the carbon nanotubes type in water solution. To confirm the suitability of these conclusions, both solutions were additionally analyzed by

conventional optical methods. The spectral distribution of absorbance versus wavelength was obtained, Fig.6. It is well known, that absorbance of semiconductor tubes corresponds to optical transitions between Van Hove singularities of valence and conducting bands. Optical absorption measurements give characteristic peaks of individual chiralities superimposed on the plasmon background. As can be seen the absorption spectra for the solution with SG 65 is characterized by peaks near $\lambda_1 = 1000$ nm (S_{11}) and $\lambda_2 = 550$ nm (S_{22}), Fig.6 a). These peaks clearly show the presence of semiconductor nanotubes (6, 5) in the solution [8]. The spectra for CG 200 does not show the peculiarities with the exception of peak near $\lambda_1 = 750$ nm (M_{11}) which can be attributed to the metal fractions, Fig.6 b). Additionally, standard PL measurements were applied in a wide range of excitation energy (300-800nm). The typical results are presented in Fig.7. As can be concluded from analysis of PL maps, the maximum of photoluminescence $\lambda_l = 980$ nm is observed for the SG 65 solution. This maximum corresponds to “band gap” energy for semiconductor nanotubes with chirality indices (6, 5) [28]. On the other hand, the spectral dependences reveal a more complex character with three emission intensity peaks for SG 65 and CG 200. Really, the peaks $\lambda_1 = 980$ nm, $\lambda_2 = 1050$, and $\lambda_3 = 1150$ nm are observed in PL maps of solutions, Fig. 7 a), b). Ideally, the photoluminescence should not be observed for the pure metallic fraction at all [1,2]. The weak residual luminescence is explained by the presence of a fraction of semiconductor tubes in the CG 200 solution in such a case. As can be seen its intensity is five times less than the values observed for the SG 65 solution. The typical Raman spectra presented by manufacturer in free access have been also considered and analyzed. The degree of G mode splitting between modes G^+ (associated with atomic vibrations along the tube axis) and G^- (vibrations normal to the tube axis) should be significantly more pronounced for product enriched in semiconductor tubes than for product enriched in metallic tubes [9]. The degree of splitting in our case is ~ 10 for SG 65 whereas this splitting is ~ 2 for CG 200 that confirm properties of these products. In general, the optical approaches appear convincing for the characterization of the carbon nanotubes type. These approaches are widely used for both express and detailed (with individual chirality determination and Kataura plot) analyze. Nevertheless, new express and simple methods should be investigated as well. Hypothetically, the obtained data will complete the data of conventional

approaches. So, the development of transducer allowing the control of SWNT conductivity remains important. As it was discussed above, the deep barrier structure utilizes the effect of recombination centers recharging at the silicon interface. Such an approach provides the possibility to detect some molecules with the own or induced dipole moment. It should be noted that the photoelectric transformation principle is used in well-known light-addressable potentiometric sensors (LAPS). The deep barrier structure also implements the photoelectric transformation principle but its application has some advantages (no necessity of using the rear illumination, no main and reference electrodes, no external bias, possibility of light addressing and surface modification).

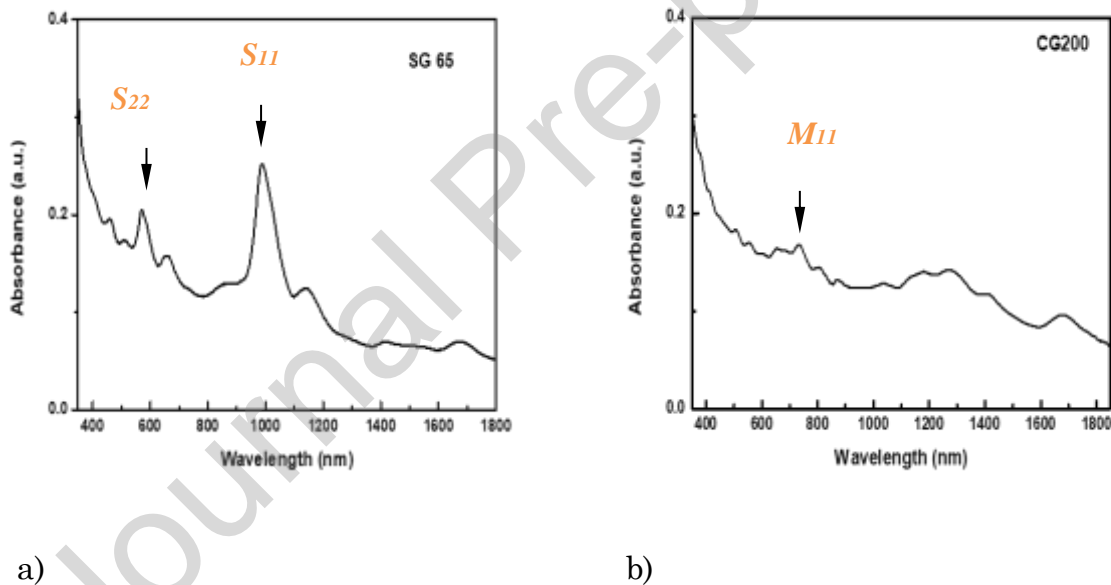


Fig.6. The absorbance spectra of the solution with SWNT of semiconductor type SG 65 (a), of metallic type CG 200 (b).

As physical transformation mechanism is different from conventional field-effect transducers, the obtained information will contain some unique and specific traits of investigated substance. This circumstance enhances the capability to recognize analytes with similar chemical structures using “electronic nose” system.

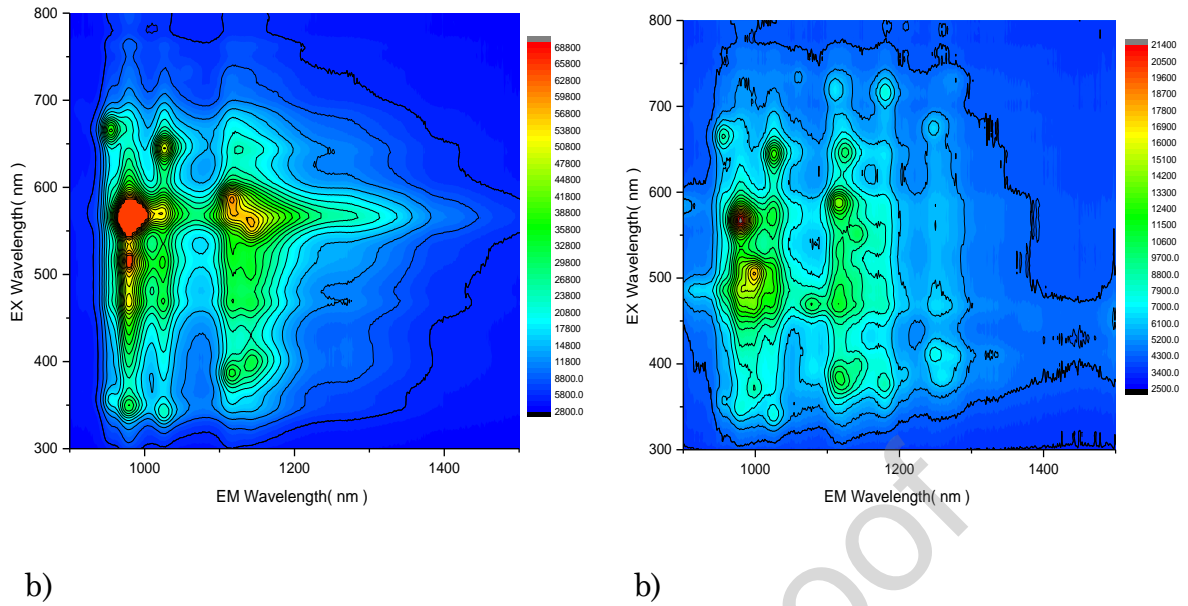


Fig. 7. The result of photoluminescence measurements for two SWNT solutions: semiconductor type SG 65 (a), of metallic type CG 200 (b).

3.3 Physical analysis and verification of the sensor model

Let us analyze in detail the physical peculiarities of the results represented in Fig. 5 b) c). To explain these experimental results some structural and chemical aspects should be taken into account [11, 12]. The sensor surface contacts with analytes like SWNT/(SDBS)/water. The molecule of SDBS anionic surfactant consists of two parts: hydrophilic polar head group (sodium sulfonate) and a non-polar hydrophobic tail (benzene ring and dodecane), Fig.8.

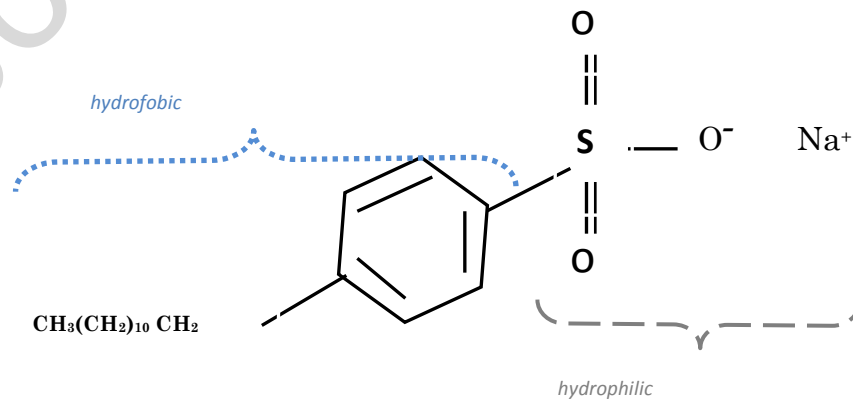


Fig. 8 The chemical structure of SBDS molecules.

The spatial configuration of molecular structures with pronounced dipole moments should influence the recombination process at the sensor surface. The principal interaction with the tube surface is implemented via hydrophobic tails. It is considered that both benzene ring (due to π - π stacking) and dodecane tails (due to "rigidity" of CH_2 chain) provide high dispersive ability [[29],[30],[31]]. Conversely, hydrophilic groups protrude into the water "protecting" the hydrophobic surface of the carbon tube. The polarizability and static dielectric constant of the metallic tube is much larger than the semiconductor one. As adsorption of surfactant at the tube surface is controlled by electrostatic interactions (van der Waals forces, dipole-dipole interactions), two hypotheses can be put forward 1) the spatial distributions of adsorbed SDBS fragment is different for metallic and semiconductor tube; 2) the adsorbed fragments, wrapping carbon tubes, induce the different electric fields. Some interesting details concerning the spatial distribution of adsorbed surfactants were obtained with all-atom molecular dynamics simulations in [29]. Taking into account the physical adsorption of surfactant molecules, the variety was analysed of energetically favourable configurations. When coverage is low, the surfactant molecules tend to orient parallel to the tube axis. The surfactant tails and most benzene rings are close to the nanotube surfaces, while most of the head groups are slightly protruded into water. The Na^+ ions accumulate near sulfonate groups, maintaining the hydration water. As the surface coverage increases, the surfactant head groups protrude toward the aqueous phase, pulling the benzene rings, away from the surface. It was predicted that surfactant molecules tend to form self-assembled disordered aggregates or micelle on the tube surface in some cases. The morphology of such aggregates depends on the conductivity type, coverage and tube diameter. Thus, electrostatic influence on recombination parameters of silicon surface is appearing to be different for SG 65 and CG 200.

The strict calculation of recombination velocity, for a certain semiconductor surface, requires the understanding of the energy dependence of interface state density and capture cross-sections. The parameters of the interface (SiO_2/Si or some other) depend on the individual surface treatment and thus have to be determined experimentally. Let us make the assumption that contact with each solutions affects only the band bending near surface, whereas cross-sections, values of energy concentration of recombination centers remain unchanged, this case is shown in

Fig.3. The proposed model allows us to perform the calculation of the photocurrent i_{ph} versus band surface band bending Y_s , according to the expressions (1) and (5). It was established [27] that levels close to the mid gap (from the range $E_i \pm 0.2$ eV) usually determine the recombination process at the interface SiO_2/Si for the thermally oxidized surface. So we can choose such value of energy for calculation of photocurrent through deep silicon structure in model approach. The values of recombination parameters used in calculation where $\sigma_n=\sigma_p=10^{-17}cm^2$ and $E_{ti}=2kT=0.05eV$.

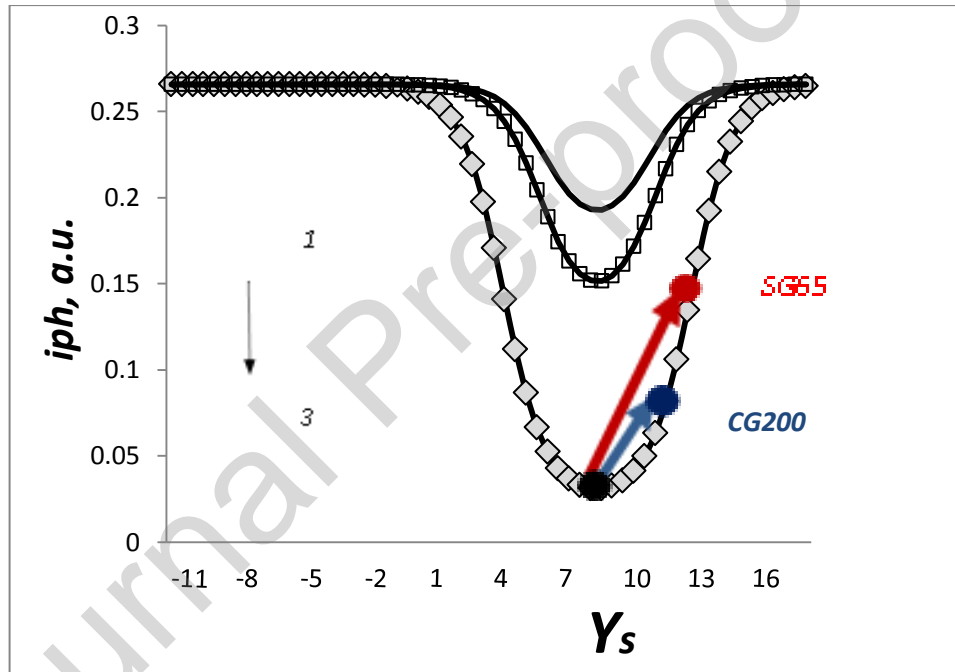


Fig. 9 The calculated photocurrent values versus pre surface band bending for, $N_t = 10^9 cm^{-2}$, $s_{max} = 5000 cm/s$ (1), $N_t = 10^{10} cm^{-2}$, $s_{max} = 10000 cm/s$ (2), $N_t = 10^{11} cm^{-2}$, $s_{max} = 100000 cm/s$ (3).

The maximums of recombination velocity were evaluated from expression (4) as $S_{max} \sim \sigma_n N_t v(p_o/n_i) / (1 + ch((E_{ti}/kT))$. The N_t concentration was varied in its typical range from $10^9 cm^{-2}$ to $10^{11} cm^{-2}$, curves 1-3 respectively. The dependences of $i_{ph}(Y_s)$ obtained for different concentration of the recombination centers at the working interface are presented in Fig.9. It can be seen that a minimum of photocurrent is achieved for the band bending that corresponds to the maximum of surface

recombination velocity, Fig.3. The proposed model qualitatively explains the difference between 2D photocurrent distributions. As the local electric field near the silicon surface is different for SG65 and CG 200, the initial band-bending can be changed differently. The latter involves the different value of photocurrent and allows recognition of metallic and semiconductor tubes. It is supposed, for more certainty, that initial band bending corresponds to a minimum of photocurrent (maximum of recombination), i.e. $Y_{o\ max} = 9kT$. The red and the blue arrows in Fig.9 (curve 3) indicate the possible shifts of initial band bending due to the electrostatic factor. As can be seen, the increase of band bending from $9kT$ to $13kT$ leads to 0.15/0.05~3 ratio of photocurrents for semiconductor type whereas the increase of band bending from $9kT$ to $11kT$ leads to 0.12/0.05~2 ratio of photocurrents for metallic type. As can be concluded, the average ratios I_{ph}^{cg200}/I_{ph} , I_{ph}^{sg65}/I_{ph} obtained from the experiment are close to the values calculated in the modeling approach for $N_t \sim 10^{11}$ cm⁻².

To summarize, we can state that adsorption of the surfactant at the surface of metallic and semiconductor nanotube can modify their electrical properties in a specific way. The deep barrier sensory structure is shown to be sufficiently sensitive to recognize the local electric field associated with such molecular structures. That is why the proposed transducer can be regarded as a promising base for the development of a new non-destructive and technically simple method of SWNTs type control. The pros are: 1) express and high sensitive method, only small volume is needed (the optical methods [[1],[2],[28],[33]] require sufficiently complex and expensive set-up whereas the investigation of transport properties of SWNT-based FET structures at different temperature requires additional technological steps [9,16]); 2) simple and compact realization of sensory structure, instead of scanning laser beam the LED matrix can be used; 3) obtained data will complete the conventional methods requiring complex expensive set-up. The possible con is high requirement to surface and silicon interface stability. Some additional investigations are needed to clarify the interaction of an SWNT solution with the silicon surface. Our calculation shows that a higher concentration of centers allows obtaining a higher change of photocurrent i_{ph} due to electrostatic influence on surface band-bending, Fig.9. It can be noticed, on the other hand, that if the concentration is too high ($N_t \geq 10^{12}$ cm⁻²) a specific “fixation” of the E_f Fermi level

near the silicon surface is possible. This aspect evidently limits the efficiency of the recombination sensor. The thin passivation film is believed to allow avoiding the fixation of Fermi [32]. The adsorption efficiency of sensory structure can be also increased in such a way but the issue requires further examination.

4, CONCLUSIONS

It was revealed that the silicon sensory structure based on the deep barrier is appropriate for the recognition of water solutions of metallic and semiconductor SWNT covered with surfactant (SDBS). The proposed sensory structure, different from the conventional light addressable potentiometric sensor, implements a new photovoltaic conversion principle. The photocurrent collected from the deep silicon barrier depends significantly on surface recombination when light with high absorption coefficient is used. The photocurrent analytical dependence on surface band bending has been evaluated for the first time. The recognition of SWNT is attributed to specific electrostatic influence (defined by locally induced dipole moment) on the parameter of recombination centers at silicon interface and surface band bending. The experimental results can be qualitatively explained in the frame of Stevenson-Keyes theory taking into account the dielectric properties of metallic and semiconductor tubes. The different values of polarizability involve peculiarities of adsorption and distribution of surfactant molecules at the tube surface. Based on the reported results, a new SWNT conductivity control method can be developed. This method allows completing the data received from the photoluminescence and optical absorption measurement.

ACKNOWLEDGMENT

This work was supported by EU Horizon 2020 Research and Innovation Staff Exchange Programme (RISE) under Marie Skłodowska-Curie Action (project 690945 “Carther” and project 101008159 “UNAT”)

REFERENCES

- [1]. H. Kataura et al. Optical properties of single-wall carbon nanotubes *Synthetic metals*, 103 (1999), pp. 2555-2558
- [2]. R. Saito, G. Dresselhaus, M. S. Dresselhaus *Physical properties of carbon nanotubes*. – 1998
- [3]. J. Kong J. et al. Nanotube molecular wires as chemical sensors *Science*, 287(2000), pp. 622-625
- [4]. A. Jain, A. Homayoun, C. Bannister CW, et al. Single-walled carbon nanotubes as near-infrared optical biosensors for life sciences and biomedicine *Biotechnol J.*, 10(2015), pp. 447–459
- [5]. A. D. Slattery, C.J. Shearer, J.G. Shapter, J.S. Quinton, C.T. Gibson Improving resolution and function of scanning probe microscopes. Solution based methods for the fabrication of carbon nanotube modified atomic force microscopy probes *Nano materials*, 7 (2017), p. 346(1-13).
- [6]. T.S. Grace, C.T. Gibson, J.R. Gascooke, J.G. Shapter The Use of Gravity Filtration of Carbon Nanotubes from Suspension to Produce Films with Low Roughness for Carbon Nanotube/Silicon Heterojunction Solar Device Application *Applied Sciences* 10 ,(2020), p. 6415 (1-18)
- [7]. Mohd Norizan, Muhammad, Harussani Moklis, Siti Zulaikha Ngah Demon^a, Norhana Abdul Halim, Alinda Samsuri^a, Imran Syakir Mohamad, Victor Feizal Carbon nanotubes: functionalisation and their application in chemical sensors, *RSC Adv.*, 10(2020), pp 43704-43732
- [8]. J. Jiang J. et al. Chirality dependence of exciton effects in single-wall carbon nanotubes: Tight-binding model /*Physical Review B.*, 75 (2007), pp. 035407 1-13.
- [9]. G. Samsonidze, R. Saito, A. Jorio,, M. A. Pimenta, A. G. Souza F, A. Grüneis, G. Dresselhaus, M. S. Dresselhaus. The concept of cutting lines in carbon nanotube science *Journal of Nanoscience and Nanotechnology (Review)*, 3(2003), pp. 431-458
- [10]. M. E. Roberts, M. C. LeMieux, Z. Bao Sorted and aligned single-walled carbon nanotube networks for transistor-based aqueous chemical sensors *Acs Nano.*, 10(2009), pp. 3287-3293

- [11]. A.J. Blanch, C.E. Lenehan, J.S. Quinton Optimizing surfactant concentrations for dispersion of single-walled carbon nanotubes in aqueous solution *The Journal of Physical Chemistry B*, 114 (2010), pp. 9805-9811
- [12]. Boris I. Kharisov, Oxana V. Kharissova, Alejandro Vázquez Dimas Dispersion, solubilization and stabilization in “solution” of single-walled carbon nanotubes, *RSC Adv.*, 6(2016), pp. 68760-68787
- [13]. Constantine Y Khripin, Jeffrey A. Fagan, and Ming Zheng Spontaneous partition of carbon nanotubes in polymer-modified aqueous phases, *J Am Chem Soc* 135(2013), pp. 6822-6827.
- [14]. Fushen Lu, Mohammed J. Meziani, Li Cao and Ya-Ping Sun Separated Metallic and Semiconducting Single-Walled Carbon Nanotubes: Opportunities in Transparent Electrodes and Beyond, *Langmuir* 27(2011), pp. 4339–4350
- [15]. H. W. Lee et al. Selective dispersion of high purity semiconducting single-walled carbon nanotubes with regioregular poly(3-alkylthiophene)s, *Nature communications*, 2(2011),pp.541-549.
- [16]. L. Wei et al. (9,8) Single-walled carbon nanotube enrichment via aqueous two-phase separation and their thin-film transistor applications *Advanced Electronic Materials*, 11(2015),pp. 150051 1-8
- [17]. G. Hong et al. Separation of Metallic and Semiconducting Single-Walled Carbon Nanotube Arrays by “Scotch Tape” *Angewandte Chemie International Edition*, 50 (2011), pp. 6819-6823
- [18]. S.V. Litvinenko A.V. Kozinetz, V. A Skryshevsky Concept of photovoltaic transducer on a base of modified p-n junction solar cell, *Sensors and Actuators A: Physical* 224(2015), pp. 30-35
- [19]. A.V. Kozinetz, S.V. Litvinenko Physical properties of sensor structures on the basis of silicon p-n junction with interdigitated back contacts *Ukrainian Journal of Physics* 57(2012),pp.1234-1238
- [20]. Anton I. Manilov, Aleksey V Kozinetz, Sergiy V Litvinenko, Valeriy A Skryshevsky, Mohammed Al Araimi, Alex Rozhin Effect of nano-carbon dispersions on signal in silicon-based sensor structure with photoelectrical transducer principle, *Current Applied Physics* 9 (2019), pp. 308-313
- [21]. Tao Jiang, C. A. Amadei, N. Gou, Y.Lin, J. Lan, Chad Vecits and April Z . Gu Toxicity of single-walled carbon nanotubes (SWCNTs): effect of lengths, functional groups and electronic structures revealed by a quantitative toxicogenomics assay

- Environ. Sci.Nano, **7**(2020),pp. 1348-1364
- [22]. Arul Prakach Francis, Thiyagarajan Devasena Toxicity of carbon nanotubes: A review Toxicology and industrial health, **34**(2018),pp. 200-210
- [23]. Debashish Mohanta, Soma Patnaik, Sanchit Sood, Nilanjan Da Carbon nanotubes: Evaluation of toxicity at biointerfaces Journal of Pharmaceutical Analysis, **9**(2019), pp. 293-300
- [24]. K. Dasgupta, J. B. Joshi, S. Banerjee Fluidized bed synthesis of carbon nanotubes – A review Chem. Eng.J.,**171**(2011), pp. 841-869 <https://doi.org/10.1016/j.cej.2011.05.038>
- [25]. I. Swyzer, R. Kaegi, L. Sigg, B. Nowack Colloidal stability of suspended and agglomerate structures of settled carbon nanotubes in different aqueous matrices, Water Res. **47** (2013) p. 3910
- [26]. T. Stevenson R.J. Keyes, *Physica*, **20**(1954) Measurement of recombination velocity at germanium surface, pp. 1041-1046. [https://doi.org/10.1016/S0031-8914\(54\)80229-1](https://doi.org/10.1016/S0031-8914(54)80229-1)
- [27]. Armin G. Aberle, Stefan Glutz and Wilhelm Warta Impact of illumination level and oxide parameters on Shockley-Read-Hall recombination at the Si-SiO₂ interface J. Apply Physics, **71**(1992), pp. 4422-4431
- [28]. S. M. Bachilo Structure-assigned optical spectra of single-walled carbon nanotubes Science, **298**(2002), pp. 2361-2366
- [29]. Manaswe Suttipongand, Alberto Striolo at al. Equimolar of aqueos linear and Branched SDBS surfactant simulated on single walled carbon nanotubes RSC Advanced, **5**(2015),pp. 900460-900490
- [30]. Kuripin C. Y., Fagan J. A., Zheng M. Spontaneous partition of carbon nanotubes in aquaeus phases Journal of the American Chemical Society, **135**(2013),pp.6822-6825
- [31]. H. Gui Redox sorting of carbon nanotubes Nanoletters, **16**(2015),pp.1642-1646
- [32]. N.A. Davidenko, O.V. Tretyak, N.G. Chuprina, Y.P. Dehtarenko, A.A. Ischenko, A.V. Kozinetz, V.A. Skryshevsky Sensitization of photoconducting properties of holographic recording media based on glycidylcarbazole cooligomers by organic dyes Molecular Crystals and Liquid Crystals, **535**(2011), pp. 148-155 DOI: 10.1080/154211406.2011.537969
- [33]. A. Jorio Characterizing carbon nanotube samples with resonance Raman

scattering *New Journal of Physics*, 5 (2003),pp. 139.1-139.17

biography

A.V. Kozinetz received his Ph.D. in 2007 (candidate of physics and mathematics sciences). He graduated from radiophysics faculty, Taras Shevchenko National University of Kyiv in 1996. He is now researcher of laboratory of Institute of High Technologies of this university. Fields of research are solar cell physics, chemical sensors and semiconductor materials

S.V. Litvinenko graduated from radiophysics faculty, Taras Shevchenko National University of Kyiv in 1978, received his Ph.D. in 1988 (candidate of physics and mathematics sciences). Now he is a head o research group of Institute of High Technologies of this university. Fields of research are photovoltaics, hydrogen energy, chemical sensors and semiconductor materials.

V.A. Skryshevsky received his Ph.D. degree in 1984, and his Doctor of Science degree (Habilitation) in 2001 at Taras Shevchenko National University of Kyiv. Skryshevsky is currently professor and Head of Department of Nanophysics of Condensed Matters at Institute of High Technologies, Taras Shevchenko National University of Kiev. His main scientific and research interests include the micro- and nano-technology, optoelectronics, solar cells, hydrogen energy, chemical and bio-sensors.

A.V. Kozinetz received his Ph.D. in 2007 (candidate of physics and mathematics sciences). He graduated from radiophysics faculty, Taras Shevchenko National University of Kyiv in 1996. He is now researcher of laboratory of Institute of High Technologies of this university. Fields of research are solar cell physics, chemical sensors and semiconductor materials

S.V. Litvinenko graduated from radiophysics faculty, Taras Shevchenko National University of Kyiv in 1978, received his Ph.D. in 1988 (candidate of physics and mathematics sciences). Now he is a head o research group of Institute of High Technologies of this university. Fields of research are photovoltaics, hydrogen energy, chemical sensors and semiconductor materials.

V.A. Skryshevsky received his Ph.D. degree in 1984, and his Doctor of Science degree (Habilitation) in 2001 at Taras Shevchenko National University of Kyiv. Skryshevsky is currently professor and Head of Department of Nanophysics of Condensed Matters at Institute of High Technologies, Taras Shevchenko National University of Kiev. His main scientific and research interests include the micro- and nano-technology, optoelectronics, solar cells, hydrogen energy, chemical and bio-sensors.

Declaration of interests

- The authors declare that they have no known competing financial interests or personal relationships that could have appeared to influence the work reported in this paper.
- The authors declare the following financial interests/personal relationships which may be considered as potential competing interests:

Highlights

- **The model of sensory structure based on a deep silicon barrier (recombinational transducer) has been developed.**
- **The recombinational transducers are appropriate for the recognition of metallic and semiconductor single-wall carbon nanotubes.**
- **The adsorption of surfactant molecules at the tube surface of metallic and semiconductor single-wall nanotubes modifies their dielectric properties.**
- **The dependences of photocurrent on pre-surface band bending are calculated for sensory structure based on deep silicon barrier.**